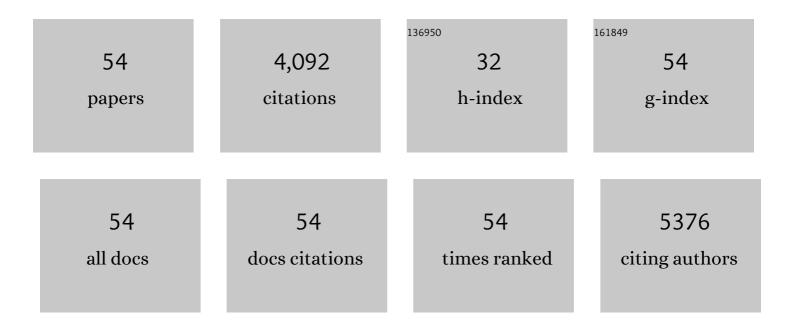


List of Publications by Year in descending order

Source: https://exaly.com/author-pdf/7404503/publications.pdf Version: 2024-02-01



KEVANILI

#	Article	IF	CITATIONS
1	Estimation of Electronegativity Values of Elements in Different Valence States. Journal of Physical Chemistry A, 2006, 110, 11332-11337.	2.5	576
2	High-Density Ultra-small Clusters and Single-Atom Fe Sites Embedded in Graphitic Carbon Nitride (g-C ₃ N ₄) for Highly Efficient Catalytic Advanced Oxidation Processes. ACS Nano, 2018, 12, 9441-9450.	14.6	455
3	Electronegativity Identification of Novel Superhard Materials. Physical Review Letters, 2008, 100, 235504.	7.8	297
4	Facile synthesis of morphology and size-controlled zirconium metal–organic framework UiO-66: the role of hydrofluoric acid in crystallization. CrystEngComm, 2015, 17, 6434-6440.	2.6	200
5	Crystallization design of MnO2 towards better supercapacitance. CrystEngComm, 2012, 14, 5892.	2.6	187
6	Solvothermal synthesis of NH ₂ -MIL-125(Ti) from circular plate to octahedron. CrystEngComm, 2014, 16, 9645-9650.	2.6	187
7	Microwave–Hydrothermal Crystallization of Polymorphic MnO ₂ for Electrochemical Energy Storage. Journal of Physical Chemistry C, 2013, 117, 10770-10779.	3.1	168
8	Synthesis of Fe/M (M = Mn, Co, Ni) bimetallic metal organic frameworks and their catalytic activity for phenol degradation under mild conditions. Inorganic Chemistry Frontiers, 2017, 4, 144-153.	6.0	131
9	Interfacial charge transfer in 0D/2D defect-rich heterostructures for efficient solar-driven CO2 reduction. Applied Catalysis B: Environmental, 2019, 245, 760-769.	20.2	118
10	Self‣upporting 3D Carbon Nitride with Tunable n → π* Electronic Transition for Enhanced Solar Hydrogen Production. Advanced Materials, 2021, 33, e2104361.	21.0	105
11	Magnetic ordered mesoporous Fe 3 O 4 /CeO 2 composites with synergy of adsorption and Fenton catalysis. Applied Surface Science, 2017, 425, 526-534.	6.1	98
12	In situ synthesis of titanium doped hybrid metal–organic framework UiO-66 with enhanced adsorption capacity for organic dyes. Inorganic Chemistry Frontiers, 2017, 4, 1870-1880.	6.0	96
13	Ultrathin sulfur-doped holey carbon nitride nanosheets with superior photocatalytic hydrogen production from water. Applied Catalysis B: Environmental, 2021, 284, 119742.	20.2	88
14	Defects Promote Ultrafast Charge Separation in Graphitic Carbon Nitride for Enhanced Visibleâ€Lightâ€Driven CO ₂ Reduction Activity. Chemistry - A European Journal, 2019, 25, 5028-5035.	3.3	85
15	CO ₂ Hydrogenation to Hydrocarbons over Iron-based Catalyst: Effects of Physicochemical Properties of Al ₂ O ₃ Supports. Industrial & Engineering Chemistry Research, 2014, 53, 17563-17569.	3.7	76
16	Water-soluble inorganic salts with ultrahigh specific capacitance: crystallization transformation investigation of CuCl2 electrodes. CrystEngComm, 2013, 15, 10367.	2.6	70
17	CoCl ₂ Designed as Excellent Pseudocapacitor Electrode Materials. ACS Sustainable Chemistry and Engineering, 2014, 2, 440-444.	6.7	67
18	Synthesis of magnetic porous Fe 3 O 4 /C/Cu 2 O composite as an excellent photo-Fenton catalyst under neutral condition. Journal of Colloid and Interface Science, 2016, 475, 119-125.	9.4	64

Keyan Li

#	Article	IF	CITATIONS
19	Solution-Phase Electronegativity Scale: Insight into the Chemical Behaviors of Metal Ions in Solution. Journal of Physical Chemistry A, 2012, 116, 4192-4198.	2.5	62
20	Effects of Monocarboxylic Acid Additives on Synthesizing Metal–Organic Framework NH ₂ -MIL-125 with Controllable Size and Morphology. Crystal Growth and Design, 2017, 17, 6586-6595.	3.0	55
21	High performance porous MnO@C composite anode materials for lithium-ion batteries. Electrochimica Acta, 2016, 188, 793-800.	5.2	51
22	Hardness of materials: studies at levels from atoms to crystals. Science Bulletin, 2009, 54, 131-136.	1.7	50
23	Facile synthesis of Fe-containing metal–organic frameworks as highly efficient catalysts for degradation of phenol at neutral pH and ambient temperature. CrystEngComm, 2015, 17, 7160-7168.	2.6	50
24	Surfactant-assisted synthesis of hierarchical NH ₂ -MIL-125 for the removal of organic dyes. RSC Advances, 2017, 7, 581-587.	3.6	50
25	Solar-driven CO2 conversion over Co2+ doped 0D/2D TiO2/g-C3N4 heterostructure: Insights into the role of Co2+ and cocatalyst. Journal of CO2 Utilization, 2020, 38, 16-23.	6.8	49
26	Electronegativities of Elements in Covalent Crystals. Journal of Physical Chemistry A, 2008, 112, 7894-7897.	2.5	45
27	Controlled synthesis of mixed-valent Fe-containing metal organic frameworks for the degradation of phenol under mild conditions. Dalton Transactions, 2016, 45, 7952-7959.	3.3	43
28	Group Electronegativity for Prediction of Materials Hardness. Journal of Physical Chemistry A, 2012, 116, 6911-6916.	2.5	40
29	Electronegativityâ€related bulk moduli of crystal materials. Physica Status Solidi (B): Basic Research, 2011, 248, 1227-1236.	1.5	38
30	Facile Construction of a Hollow In ₂ S ₃ /Polymeric Carbon Nitride Heterojunction for Efficient Visible-Light-Driven CO ₂ Reduction. ACS Sustainable Chemistry and Engineering, 2021, 9, 5942-5951.	6.7	37
31	A facile sulfur-assisted method to synthesize porous alveolate Fe/g-C3N4 catalysts with ultra-small cluster and atomically dispersed Fe sites. Chinese Journal of Catalysis, 2020, 41, 1198-1207.	14.0	37
32	New insight into the mechanism of enhanced photo-Fenton reaction efficiency for Fe-doped semiconductors: A case study of Fe/g-C3N4. Catalysis Today, 2021, 371, 58-63.	4.4	36
33	From chemistry to mechanics: bulk modulus evolution of Li–Si and Li–Sn alloys via the metallic electronegativity scale. Physical Chemistry Chemical Physics, 2013, 15, 17658.	2.8	34
34	Controllable assembly of single/double-thin-shell g-C ₃ N ₄ vesicles <i>via</i> a shape-selective solid-state templating method for efficient photocatalysis. Journal of Materials Chemistry A, 2019, 7, 17815-17822.	10.3	33
35	A new set of electronegativity scale for trivalent lanthanides. Physica Status Solidi (B): Basic Research, 2007, 244, 1982-1987.	1.5	28
36	Metal–Organic Framework-Derived Tubular In ₂ O ₃ –C/CdIn ₂ S ₄ Heterojunction for Efficient Solar-Driven CO ₂ Conversion. ACS Applied Materials & Interfaces, 2022, 14, 20375-20384.	8.0	26

Keyan Li

#	Article	IF	CITATIONS
37	BAND GAP ENGINEERING OF CRYSTAL MATERIALS: BAND GAP ESTIMATION OF SEMICONDUCTORS VIA ELECTRONEGATIVITY. Functional Materials Letters, 2012, 05, 1260002.	1.2	25
38	New development of concept of electronegativity. Science Bulletin, 2009, 54, 328-334.	9.0	24
39	Facile and green synthesis of TiN/C as electrode materials for supercapacitors. Applied Surface Science, 2019, 470, 241-249.	6.1	22
40	SITE SELECTIVITY IN DOPED POLYANION CATHODE MATERIALS FOR Li -ION BATTERIES. Functional Materials Letters, 2013, 06, 1350043.	1.2	19
41	Surfactant-assisted crystallization of porous Mn ₂ O ₃ anode materials for Li-ion batteries. CrystEngComm, 2015, 17, 5094-5100.	2.6	19
42	BAND GAP PREDICTION OF ALLOYED SEMICONDUCTORS. Functional Materials Letters, 2011, 04, 217-219.	1.2	18
43	An S-scheme heterojunction constructed from α-Fe ₂ O ₃ and In-doped carbon nitride for high-efficiency CO ₂ photoreduction. Catalysis Science and Technology, 2022, 12, 1520-1529.	4.1	16
44	Solution reaction design: electroaccepting and electrodonating powers of ions in solution. Nanoscale Research Letters, 2012, 7, 6.	5.7	15
45	Effect of Electrostatic and Size on Dopant Occupancy in Lithium Niobate Single Crystal. Inorganic Chemistry, 2013, 52, 10206-10210.	4.0	15
46	A rapid combustion route to synthesize high-performance nanocrystalline cathode materials for Li-ion batteries. CrystEngComm, 2014, 16, 10969-10976.	2.6	15
47	Facile synthesis of iron-based compounds as high performance anode materials for Li-ion batteries. RSC Advances, 2014, 4, 36507.	3.6	15
48	Evolution of Surface Oxidation on Ta ₃ N ₅ as Probed by a Photoelectrochemical Method. ACS Applied Materials & Interfaces, 2021, 13, 17420-17428.	8.0	12
49	Crystallization behavior of 3D-structured OMS-2 under hydrothermal conditions. CrystEngComm, 2015, 17, 3636-3644.	2.6	11
50	Facile synthesis of magnetic Fe ₃ O ₄ /CeCO ₃ OH composites with excellent adsorption capability for small cationic dyes. RSC Advances, 2015, 5, 94397-94404.	3.6	11
51	Solvothermal synthesis of 3D hierarchical Cu2FeSnS4 microspheres for photocatalytic degradation of organic pollutants. Environmental Research, 2022, 205, 112539.	7.5	7
52	Nitrogen-rich porous polymeric carbon nitride with enhanced photocatalytic activity for synergistic removal of organic and heavy metal pollutants. Environmental Science: Nano, 2022, 9, 2388-2401.	4.3	6
53	Synthesis of spinel LiMn2O4 cathode material by a modified solid state reaction. Functional Materials Letters, 2015, 08, 1540002.	1.2	5
54	Influence of surfactant-assisted synthesis and different operational parameters on photocatalytic performance of Cu2FeSnS4 particles. Surfaces and Interfaces, 2021, 24, 101134.	3.0	5